First-principles calculations of structural, electronic, and thermodynamic properties of $ZnO_{1-x}S_x$ alloys

Muhammad Zafar†, Shabbir Ahmed, M. Shakil, and M. A. Choudhary

Simulation Laboratory, Department of Physics, The Islamia University of Bahawalpur, 63100, Pakistan

(Received 26 December 2013; revised manuscript received 4 May 2014; published online 20 August 2014)

In this study the pseudo-potential method is used to investigate the structural, electronic, and thermodynamic properties of $ZnO_{1-x}S_x$ semiconductor materials. The results show that the electronic properties are found to be improved when calculated by using LDA + U functional as compared with local density approximation (LDA). At various concentrations the ground-state properties are determined for bulk materials ZnO, ZnS, and their tertiary alloys in cubic zinc-blende phase. From the results, a minor difference is observed between the lattice parameters from Vegard's law and other calculated results, which may be due to the large mismatch between lattice parameters of binary compounds ZnO and ZnS. A small deviation in the bulk modulus from linear concentration dependence is also observed for each of these alloys. The thermodynamic properties, including the phonon contribution to Helmholtz free energy ΔF, phonon contribution to internal energy ΔE, and specific heat at constant-volume C_V, are calculated within quasi-harmonic approximation based on the calculated phonon dispersion relations.

Keywords: first principles calculations, density functional theory (DFT), semiconductor materials, structural, electronic, and thermal properties

PACS: 61.72.uj, 73.20.At **DOI:** 10.1088/1674-1056/23/10/106108

1. Introduction

Wide band gap semiconductor materials are interesting due to their promising technological applications in electronic and optoelectronic devices, catalysts, chemical sensors, blue-ultraviolet light-emitting diodes, cosmetics, and pharmaceutical lotions.[1–4] They have also been found to have applications in short wave length optoelectronic components in laser diodes (LDs) and light emitting diodes (LEDs).[5] Therefore, wide band gap II–VI semiconductors have appeared as research candidates in theoretical and experimental fields.[6] Zinc oxide, a wide gap semiconductor, has potential applications in geophysical and fundamental material physics due to its stability at ambient pressure.[7] Both compounds, that is, ZnO (3.2 eV) and ZnS (3.6 eV),[8] each with zinc-blende (B3) phase are direct band gap materials and they have normally been used in ultra violet (UV)-based optoelectronic devices. The enormous number of applications of these semiconductors in optoelectronic devices are due to their wide band gaps and other unique features, such as high binding energy and thermal stability. To develop highly efficient, blue, green, and UV emitters and sensors based on these two materials, it is necessary to modify them in such a fashion that they may cover a full spectrum of band gap energies, from visible to UV. Thus, in order to obtain the full spectra of band gap energies, a systematic replacement of oxygen (O) atom by sulfur (S) in ZnO or S by O in ZnS is carried out. It is envisaged that a systematic and controlled partial replacement of O by S can modify the physical properties gradually, so that a full spectrum of band gap energies may be obtained.[9]

It is important to mention that a suitable characterization of the thermodynamic properties, such as heat capacity, Helmholtz free energy, internal energy, and entropy, are vital for enhancing the quality of electronic devices. Therefore, a good understanding of these properties is essential for the useful applications of these alloys over an extended range of pressures and temperatures. The main objective of this work is to explore the structural, electronic, and the thermodynamic properties of ZnO, ZnS, and their tertiary alloys with zinc blende phase using the pseudo-potential method in the framework of density functional perturbation theory (DFPT).

2. Computational method

All of the calculations are performed using the DFT, plane wave pseudo-potentials method, which is included in Quantum ESPRESSO,[10] using the local density approximation (LDA) exchange correlation functional given by Perdew and Zunger,[11] and ultrasoft pseudo-potential.[12] Plane wave bases set with a cutoff energy of 30 Ry are used to represent the electronic wave functions. Integration over the Brillouin zone is carried out using Monkhorst–Pack scheme[13] with $8\times8\times8$ mesh of k-points at ambient pressure for each of all $ZnO_{1-x}S_x$ compounds to attain well-converged ground state energy. The crystal unit cell of $ZnO_{1-x}S_x$ alloy is constructed using the conventional cell containing eight atoms per unit cell, in which a systematic replacement of oxygen by sulfur has been made. A Hubbard U correction[14] is included in addition to LDA to determine the electronic structure of $ZnO_{1-x}S_x$. The lattice parameters and bulk moduli of these compounds are calculated by the standard procedure of computing total energy for different volumes and is fitted to Murnaghan's equation of state.[15] The phonons calculations are performed by using linear response method[16] at Γ point. Various dynamical matrices are

†Corresponding author. E-mail: zafartariq2003@yahoo.com

© 2014 Chinese Physical Society and IOP Publishing Ltd

calculated at Γ for a $4 \times 4 \times 4$ q-points grid generated according to Monkhorst and Pack grid[13] to determine the thermal properties.

3. Results and discussion

3.1. Structural properties

To investigate $ZnO_{1-x}S_x$ alloys at $x = 0.25$, 0.5, and 0.75, we first calculate the structural properties of end binary ZnO & ZnS in B3 phase. The optimizations are performed to minimize the total energies at different lattice constants. By using the Murnaghan's equation of state (EOS),[15] equilibrium structural parameters, such as the values of the lattice parameter (a_0) and the bulk modulus (B) for binary and their tertiary alloys, are calculated. The optimized curves of $ZnO_{1-x}S_x$ alloys at $x = 0.00$, 0.25, 0.50, 0.75, and 1.00 are shown in Fig. 1, and the results are summarized in Table 1.

The present calculations of the end binaries are comparable to, and are in good agreement with, the experimental and other theoretical calculated results. The calculated lattice constants of $ZnO_{1-x}S_x$ alloys were found to increase with the increase in concentration of sulfur whereas the value of the bulk modulus decreases.

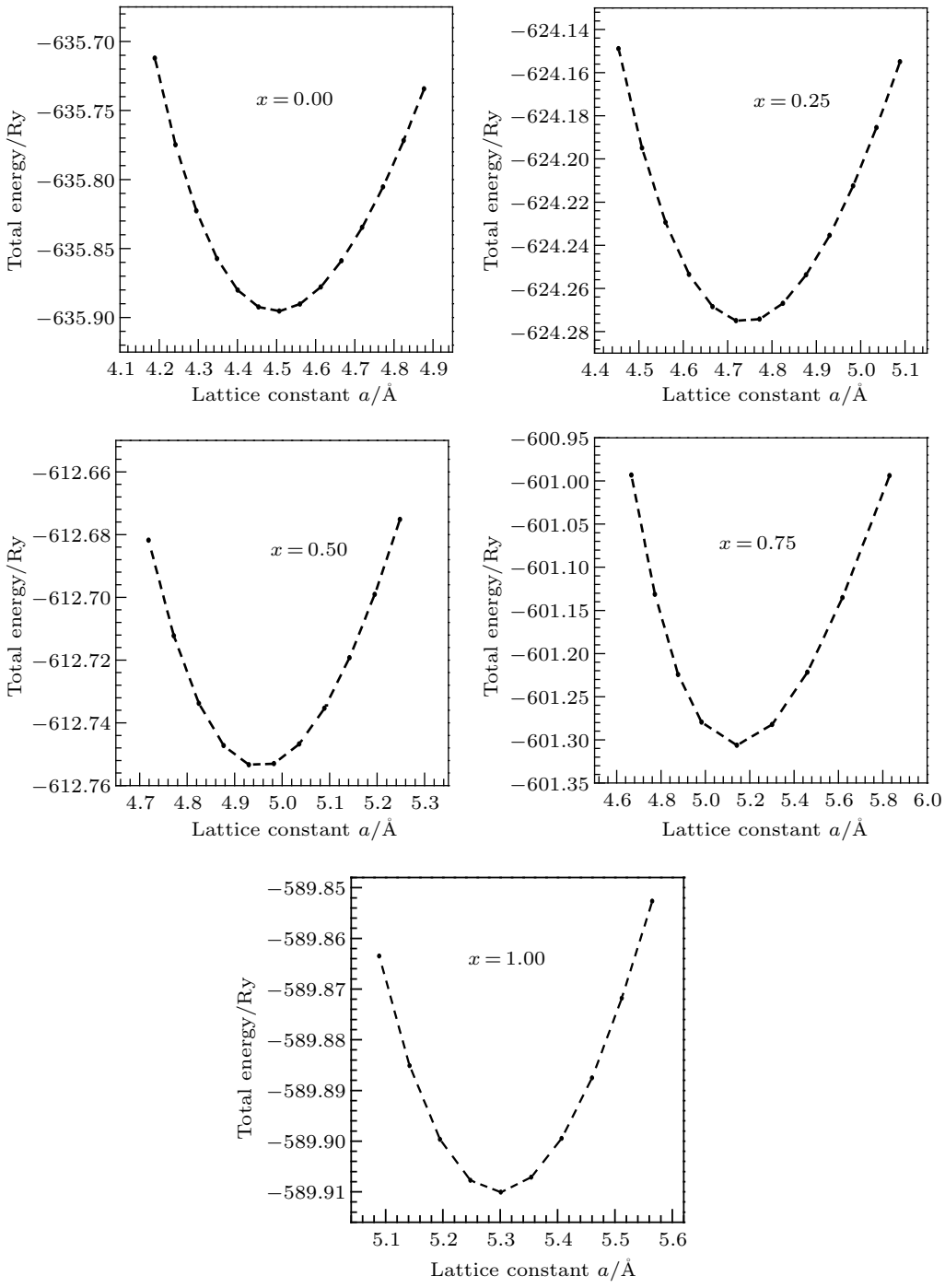


Fig. 1. Structural optimization plots for $ZnO_{1-x}S_x$ alloys at $x = 0.00$, 0.25, 0.50, 0.75, and 1.00 versus lattice constant in zinc-blende phase. The unit 1 Ry = 13.605 eV.

Table 1. Calculated lattice parameters and bulk moduli of $ZnO_{1-x}S_x$ alloys compared with experimental and theoretical results in zinc-blend (zb) structure.

Compositions	Lattice constant a_0/Å			Bulk modulus B/GPa		
x	This work	Expt.	Other calculations	This work	Expt.	Other calculations
0.00	4.50	4.62[a]	4.616[b], 4.633[c]	156.7	163.24[a]	125.34[b]
			4.623[h]			133.73[c]
						131.64[h]
0.25	4.739		126.6			
0.50	4.948		108.2			
0.75	5.142		89.9			
1.00	5.30	5.40[d]	5.34[e], 5.46[f]	84.0	75[g]	73.42[d]
						93.12[e]
						69.3[f]

[a]Ref. [17], [b]Ref. [18], [c]Ref. [19], [d]Ref. [20], [e]Ref. [21], [f]Ref. [22], [g]Ref. [23], [h]Ref. [24]

The calculated lattice constants and bulk moduli for $ZnO_{1-x}S_x$ alloys at sulfur concentration with B3 phase are presented in Fig. 2. It can be seen from the results that, with the increase in concentration of sulfur in zinc blende $ZnO_{1-x}S_x$, the lattice constants and bulk moduli show a considerable deviation from the results obtained from the Vegard's law,[25] which are comparatively large.

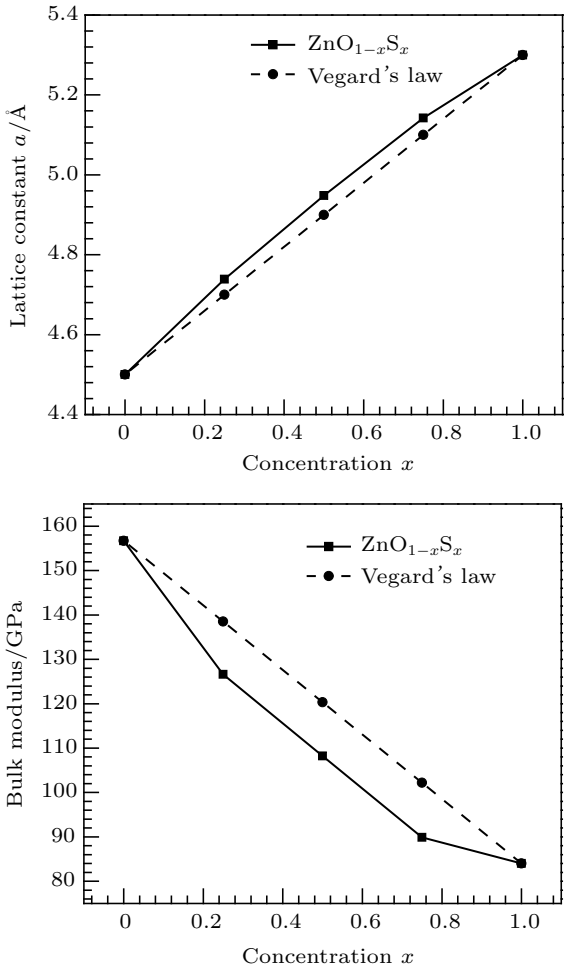


Fig. 2. Variations of the calculated lattice parameters and bulk moduli with x for $ZnO_{1-x}S_x$ alloys.

3.2. Electronic properties

The electronic band structures of materials can be used to explain most of their physical properties. To apprehend the possible technological applications of semiconductor compounds, theoretical calculations and experimental measurements are both essential. The electronic band structures of $ZnO_{1-x}S_x$ in the zinc-blende phase are studied to understand their optical significance in optoelectronic devices. The understanding of band gap and band structure is necessary for developing optoelectronic, magneto–optic, and magneto–electronic devices. In order to calculate the electronic band structure, Zn-3d, 4s, O-2s, 2p, and S-4s, 4p states are taken as valence states and all other lower states are treated as part of the core. In this study, the band gaps are calculated for $ZnO_{1-x}S_x$ along the high symmetry points at the first Brillion zone from the calculated lattice constants. In all cases, the valence band maximum (VBM) and conduction band minimum (CBM) appear at the Γ point.

Table 2. Band gap energies (eV) of $ZnO_{1-x}S_x$ in zinc-blend (zb) structure.

Compositions	Calculated	Theoretical	Theoretical	Experimental
x	LDA + U	LDA/GGA	LDA-correc[e]	
0.00	3.225	0.75[a], 0.71[b]	3.30	3.19[d]
0.25	3.468			
0.50	3.561			
0.75	3.702			
1.00	3.655	2.02[a], 2.14[b]	3.94	3.54[c]

[a]Ref. [27], [b]Ref. [26], [c]Ref. [28], [d]Ref. [29], [e]Ref. [30]

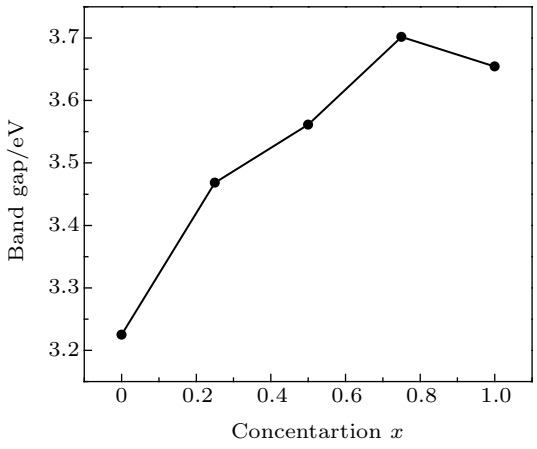


Fig. 3. Fundamental energy gap of $ZnO_{1-x}S_x$ versus concentration of sulfur in ordered alloys.

Thus, the energy gap is a direct energy gap between the top of the valence band and the bottom of the conduction band.

The obtained results are compared with other theoretical and experimental results in Table 2. With the LDA + U method (with $U = 7.5$ eV for $ZnO_{1-x}S_x$ at $x = 0.0$, 0.25, 0.50, 0.75, and $U = 5.0$ eV for ZnS) the obtained results are more consistent with experimental results, which proves that an increase in sulfur concentration x ($x = 0$, 0.25, 0.5, 0.75, 1.00) results in an increase of the energy gap, as shown in Fig. 3. The calculated band gaps of zinc-blende $ZnO_{1-x}S_x$ are consistent with the experimental values, except at very low oxygen concentration, that is, at $x = 0.75$. At a low concentration of oxygen in ZnS, the obtained band gap is high, which may be due to large size and chemical mismatch between oxygen and sulfur.[26]

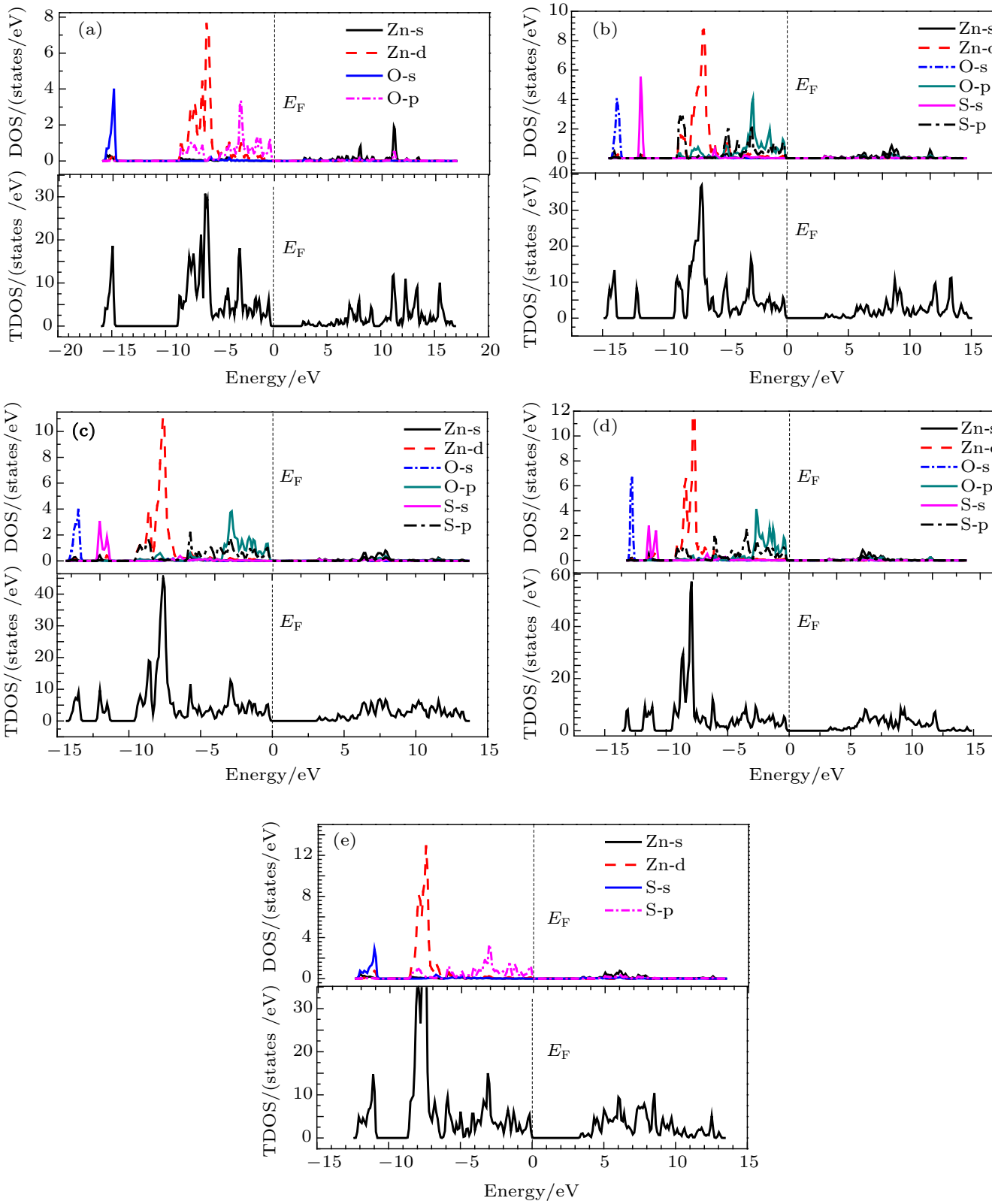


Fig. 4. (color online) Total and partial DOSs of $ZnO_{1-x}S_x$ at $x = 0.00$ (a), 0.25 (b), 0.50 (c), 0.75 (d), and 1.00 (e), each as a function of sulfur composition.

Densities of states (DOSs) for $ZnO_{1-x}S_x$ are plotted in Fig. 4, showing the total and partial DOCs in a range of −15 eV to 15 eV for $ZnO_{1-x}S_x$. The bands below the Fermi energy E_F are valence bands (VBs) and those above E_F are called conduction bands (CBs). For the case of ternary alloys, that is, $ZnO_{0.50}S_{0.50}$ and $ZnO_{0.25}S_{0.75,}$ in Figs. 4(c) and 4(d), the upper VB is dominated by O-2p and pd-hybridized states, while in the lower part of valance band the hybridization of Zn-3d and S-3p occurs. On the other hand, in Fig. 4(b), for the $ZnO_{0.75}S_{0.25}$ alloy, the upper VB is occupied by O-2p and pd-hybridized states of Zn-3d, O-2p, and S-3p. The lower part of the valance band in $ZnO_{0.75}S_{0.25}$ is occupied by a Zn-3d state. The observed conduction bands of the ternary alloys of these compounds are due to the mixed valence states. In ZnO (Fig. 4(a)), the top of the VB is caused by the Zn-3d and O-2p orbitals. In ZnS (Fig. 4(e)) the upper VB is dominated by S-3p state and the maximum peak is due to the Zn-3d state, whereas the lower band is due to the pd-hybridization of these states. In all tertiary and binary alloys, the lowest part of the VB is dominated by s states of oxygen and sulfur. As is well known, both LDA and generalized gradient approximation (GGA) calculate very small band gap because the said approximations locate the Zn-3d band incorrectly. This problem can be resolved by using the LDA + U[29–33] for the DFT calculations. From the DOS plots in Fig. 4, it is obvious that the band gap increases from $x = 0.25$ to 1.00 in $ZnO_{1-x}S_x$. This increase in band gap may be attributed to the presence of strong partial covalent bond between Zn and S as compared with between Zn and O, whereas the charge moves towards the oxygen atom because of its larger electro-negativity than S.[9]

3.3. Thermal properties

Phonons play a major role in determining the physical properties of solids, such as their thermal and electrical conductivities, superconducting temperatures, and Debye temperatures. The vibration frequency ω is a function of wave vector $\boldsymbol{q}$, which can be written with the dispersion relation $\omega = \omega_j(q)$. Since there are two atoms per unit cell in the ZB ZnO and ZnS crystal lattice, there are six branches of the phonon dispersion curve, three of which are acoustic and other three are optical. Owing to the translational symmetry $\omega_j(q+G) = \omega_j(q)$, we can calculate only the phonon frequencies in the first Brillouin zone (BZ).[34] The phonon dispersion curves at 25%, 50%, and 75% defects form complex dispersion curves. The phonon dispersion curves along some high-symmetry points (R, Γ, X, M) in the BZ are shown in Fig. 5.

All of the thermodynamic properties of materials as a function of temperature are derived by density functional perturbation theory (DFPT). These properties are usually determined by the suitable thermodynamic potential that is relevant to the given ensemble(s). In ensemble(s) where the sample specimen volume (V) and temperature (T) are independent variables, the relevant potential is the Helmholtz free energy (F). In adiabatic Born–Oppenheimer (BO) approximation, F of a semiconductor can be written as[35]

$$F = F + \Delta F = E + \Delta E - TS, \tag{1}$$

where E denotes the static contribution to the internal energy, ΔF is the phonon contribution to the Helmholtz free energy, ΔE is the contribution of the lattice vibration to the internal energy, and S is the entropy. For insulators, the electronic entropy makes no contribution to entropy; therefore, it is not included in Eq. (1). In the case of metals, this contribution is usually ignored, although it is easy to calculate. Consequently, the final quantity to calculate thermal properties is 'ΔF'. The Helmholtz free energy is usually calculated within harmonic approximation:[35]

$$\Delta F = 3nNk_{\mathrm{B}}T\int_0^{\omega_{\max}} \ln\left\{2\sinh\frac{\hbar\omega}{2k_{\mathrm{B}}T}\right\} g(\omega)\,\mathrm{d}\omega, \tag{2}$$

where k_{B} is the Boltzmann constant, n is the number of atoms per unit cell, N is the number of unit cells, ω is the phonon frequency, and $g(\omega)$ is the normalized phonon DOS. Figures 6 and 7 illustrate a relation between internal energy ΔE and molar specific heat C_V as a function of temperature (T) from 0 K to 1000 K. The internal energy ΔE and Helmholtz free energy ΔF at zero temperature represent the zero-point motion, which can be calculated from the expression

$$\Delta F_0 = \Delta E_0 = \frac{3n\int_0^{\omega_{\max}}(\hbar\omega)}{2} g(\omega)\,\mathrm{d}\omega. \tag{3}$$

By using Eq. (3), the calculated results are 12.3 kJ/mol, 4.383 kJ/mol for ZnO and ZnS, respectively. The zero-point motion contribution to the thermodynamic functions of ZnO is more important than those of ZnS, ZnSe, and ZnTe. The temperature-dependent ΔE is higher for ZnO than for ZnS, since ZnO has much higher average phonon frequency and lower entropy.[33] Within harmonic approximation, C_V is given as[35]

$$C_V = 3nk_{\mathrm{B}}T\int_0^{\omega\,\max}\left(\frac{\hbar\omega}{2k_{\mathrm{B}}T}\right)^2 \mathrm{csch}^2\left(\frac{\hbar\omega}{2k_{\mathrm{B}}T}\right) g(\omega)\,\mathrm{d}\omega. \tag{4}$$

The calculated phonon contributions to the internal energy ΔF and heat capacity for $ZnO_{1-x}S_x$, each as a function of T are presented in Figs. 6 and 7, respectively, which show that both quantities increase with the increase in temperature and concentration of sulfur. However, these quantities have almost similar values at higher temperatures. The relation of Helmholtz free energy to sulfur concentration is plotted in Fig. 8, which shows that Helmholtz free energy decreases with the increase in sulfur concentration. Zinc oxide was found to have lower C_V than the ZnS over the complete temperature range due to its DOS at low-frequency modes.[36]

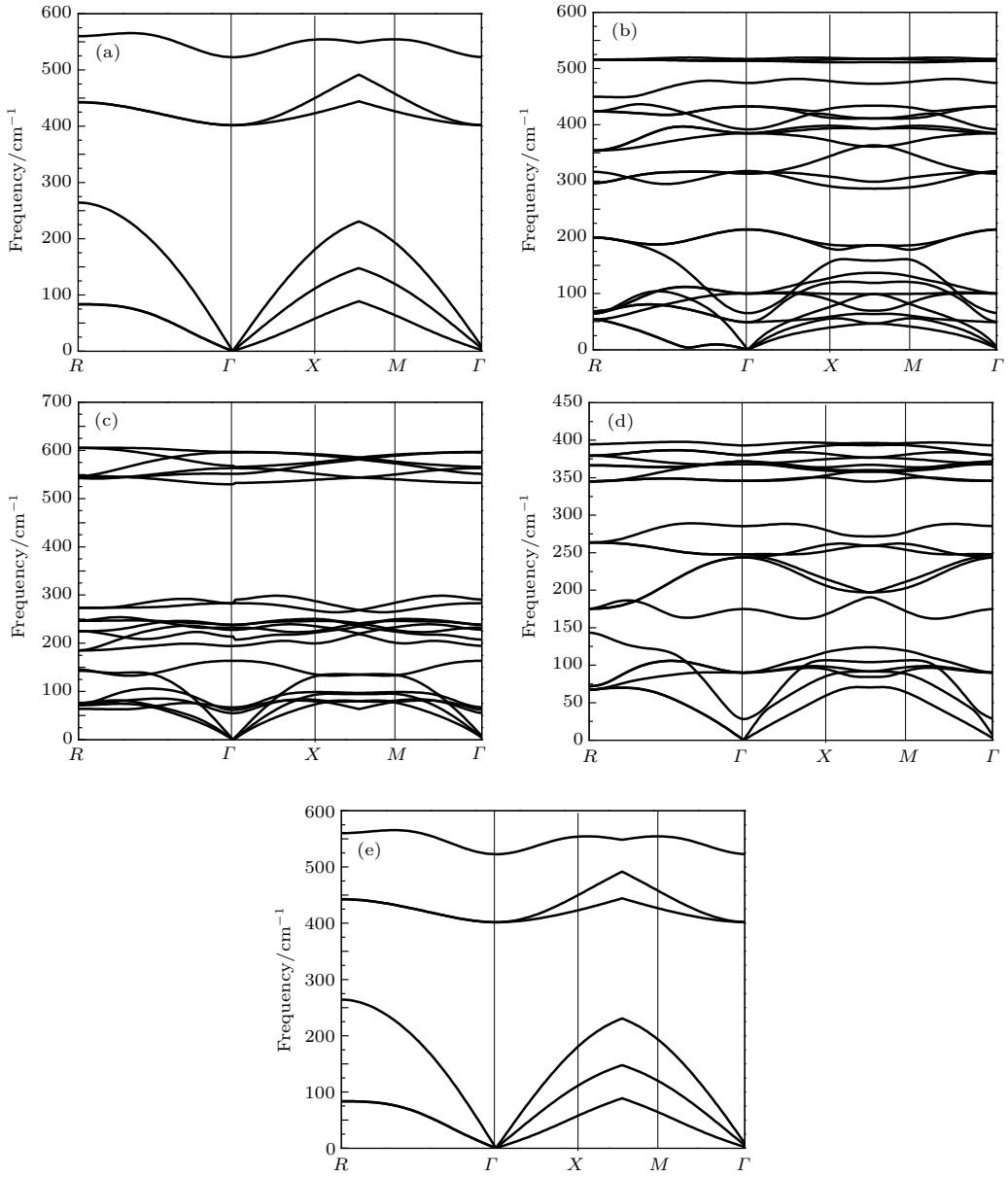


Fig. 5. Curves for the phonon dispersion of the ZB $ZnO_{1-x}S_x$ along several high-symmetry points: $x = 0.0$ (a), 0.25 (b), 0.50 (c), 0.75 (d), and 1.0 (e).

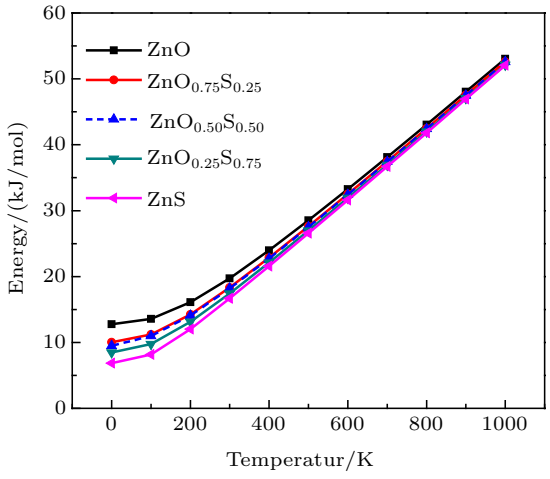


Fig. 6. (color online) Phonon contributions to the internal energy of $ZnO_{1-x}S_x$.

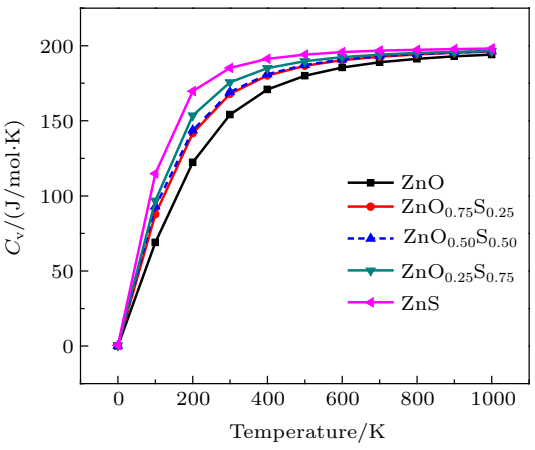


Fig. 7. (color online) Constant-volume specific heats of $ZnO_{1-x}S_x$ (per unit cell).

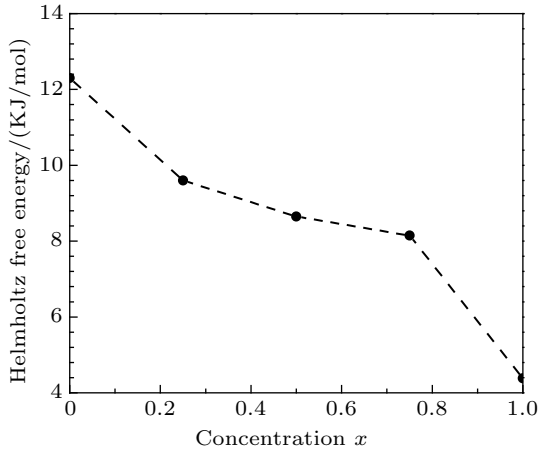


Fig. 8. Helmholtz free energy versus concentration for $ZnO_{1-x}S_x$ at zero temperature.

4. Conclusions

The pseudo-potential technique is used to calculate the electronic, structural, mechanical, and thermal properties of the $ZnO_{1-x}S_x$ alloys using the pseudo-potential method within the framework of DFT and the obtained results are compared with experimental and theoretical results. The following conclusions can be drawn from these theoretical calculations.

(i) For the zinc-blende structure of $ZnO_{1-x}S_x$, it is found that with the increase of sulfur defects the lattice constant increases from 4.50 Å to 5.30 Å whereas the bulk modulus decreases from 156.7 GPa to 84.0 GPa. The calculated band gap increases from 3.225 eV to 3.655 eV with the increase of sulfur concentration in ZnO. It is observed from the obtained results that the band gap is wide and direct for the full range concentration of sulfur.

(ii) The thermodynamic properties of $ZnO_{1-x}S_x$, including the phonon contribution to the Helmholtz free energy, the phonon contribution to the internal energy, and the constant-volume specific heat C_V, are calculated by using the quasi-harmonic approximation. The Helmholtz free energy ΔF decreases from 12.3 kJ/mol to 4.383 kJ/mol with the increase in sulfur concentration whereas internal energy and constant-volume specific heat C_V both increase. The results also show that the energy ΔE and constant-volume specific heat C_V increase as temperature increases, but both have almost constant values at high temperatures.

Acknowledgment

The authors are very grateful to Prof. M. A. Choudhary for fruitful discussion and simulation facilities in simulation laboratory at the Department of Physics, The Islamia University of Bahawalpur. The authors also thank the Higher Education Commission of Pakistan for partial funding.

References

[1] Bagnall D M, Chen Y F, Zhu Z, Yao T, Koyama S, Shen M Y and Goto T 1997 *Appl. Phys. Lett.* **70** 2230
[2] Matsuoka M 1971 *Jpn. J. Appl. Phys.* **10** 736
[3] Yu Z G, Gong H and Wu P 2006 *J. Cryst. Growth* **287** 199
[4] Kumar R S, Cornelius A L and Nicol M F 2007 *Curr. Appl. Phys.* **7** 135
[5] Cho M W, Chang J H, Bagnall D M, Koh K W, Saeki S, Park S K T, Zhu Z, Hiraga K and Yao T 1999 *J. Appl. Phys.* **85** 512
[6] Aoumeur F Z, Benkabou Kh and Belgoumene B 2003 *Physica B* **337** 292
[7] Wu H Y, Cheng X L, Hu C H and Zhou P 2010 *Physica B* **405** 606
[8] Locmelis S, Brunig C, Binnewies M, Borger A, Becker K D, Homann T and Bredow T 2007 *J. Mater. Sci.* **42** 1965
[9] Khan I and Ahmad I 2013 *Int. J. Quantum Chem.* **113** 1285
[10] Duman S, Tütüncü H M, Bağci S and Srivastava G P 2007 *AIP Conference Proceedings* **899** 247
[11] Perdew J P and Zunger A 1981 *Phys. Rev. B* **23** 5048
[12] Vanderbilt D 1990 *Phys. Rev. B* **41** 7892
[13] Monkhorst H J and Pack J D 1976 *Phys. Rev. B* **13** 5188
[14] Anisimov V I and Gunnarson O 1991 *Phys. Rev. B* **43** 7570
[15] Murnaghan F D 1944 *Proc. Natl. Acad. Sci. USA* **30** 244
[16] Baroni S, De Gironcoli S, Dal Corso A and Giannozzi P 2001 *Rev. Mod. Phys.* **73** 515
[17] Qteish A, Abu-Jafar M and Nazzal A 1998 *J. Phys.: Condens. Matter* **10** 5069
[18] Amin B, Ahmad I, Maqbool M, Ikram N, Saeed Y and Ahmad A 2010 *J. Alloys Compd.* **493** 212
[19] Karzel, Potzel H W, Kofferlein M, Schiessl W, Steiner M, Hiller U, Kalvius G M, Mitchell D W, Das T P, Blaha P, Schwarz K and Pasternak M P 1996 *Phys. Rev. B* **53** 11425
[20] Imad Khan, Iftikhar Ahmad, Rahnamaye Aliabad H A and Maqbool M 2012 *J. Appl. Phys.* **112** 073104
[21] Rabah M, Abbar B, Al-Douri Y, Bouhafs B and Sahraoui B 2003 *Mater. Sci. Eng. B* **100** 163
[22] Hassan F E H, Bleybel A, Hijazi A, Alaeddine A, Beydoun B and Zoaeter M 2007 *Mater. Lett.* **61** 1178
[23] Christensen R A and Christensen N E 1998 *Solid State Commun.* **108** 793
[24] Rashid M, Hussain F, Imran M, Ahmad S A, Noor N A, Sohaib M U and Alay-e-Abbas S M 2013 *Chin. Phys. B* **22** 087301
[25] Vegard L 1921 *Z. Phys.* **5** 17
[26] Fan X F, Shen Z X, Lu Y M and Kuo J 2009 *New J. Phys.* **11** 093008
[27] Moon C Y, Wei S H, Zhu Y Z and Chen G D 2006 *Phys. Rev. B* **74** 233202
[28] Locmelis S, Brunig C, Binnewies M, Borger A, Becker K D, Homann T and Bredow T 2007 *J. Mater. Sci.* **42** 1965
[29] Fan H, Barnard A S and Zacharias M 2007 *Appl. Phys. Lett.* **90** 143116
[30] Karazhanov S Z, Ravindran P, Grossner U, Kjekshus A, Fjellvag H and Svensson B G 2006 *J. Cryst. Growth* **287** 162
[31] Lambrecht W R L, Rodina A V, Limpijumnong S, Segall B and Meyer B K 2002 *Phys. Rev. B* **65** 075207
[32] Dong C L, Persson C, Vayssieres L, Augustsson A, Schmitt T, Mattesini M, Ahuja R, Chang C L and Guo J H 2004 *Phys. Rev. B* **70** 195325
[33] Janotti A and Walle C G V 2006 *J. Cryst. Growth* **287** 58
[34] Tan J J, Ji G F, Chen X R and Guo Q Q 2010 *Commun. Theor. Phys.* **53** 1160
[35] Maradudin A A, *et al.* 1971 *Solid State Physics*, 2nd edn., Ehrenreich H E (ed.) (New York: Academic) Chap. 4
[36] Yu Y *et al.* 2009 *Solid State Sciences* **11** 1343